Journal of Cancer Research and Clinical Oncology (2019) 145:1147–1164
https://doi.org/10.1007/s00432-019-02860-z

ORIGINAL ARTICLE – CANCER RESEARCH

CD110 promotes pancreatic cancer progression and its expression is correlated with poor prognosis

Zilong Yan[1] · Kenoki Ohuchida[1,2] · Biao Zheng[1,3] · Takashi Okumura[1] · Shin Takesue[1] · Hiromichi Nakayama[1] · Chika Iwamoto[2] · Koji Shindo[1] · Taiki Moriyama[1] · Kohei Nakata[1] · Yoshihiro Miyasaka[1] · Takao Ohtsuka[1] · Kazuhiro Mizumoto[5] · Yoshinao Oda[4] · Makoto Hashizume[2] · Masafumi Nakamura[1]

Received: 29 November 2018 / Accepted: 8 February 2019 / Published online: 15 February 2019

Abstract

Purpose This study aimed at investigating the function and significance of CD110 expression in pancreatic cancer.

Methods We performed immunohistochemical staining for CD110 expression in tumor samples from 86 patients with pancreatic cancer. We evaluated clinical outcomes and other clinicopathological factors to determine the significance of CD110 on survival and liver metastasis. We examine thrombopoietin–CD110 signaling in cancer cell extravasation in vitro and in vivo. We investigated the effects of CD110 knockdown on liver metastasis in a splenic xenograft mouse model.

Results CD110 expression in cancer cells was associated with low-histological-grade invasive ductal carcinoma, and patients with high CD110 expression had poorer prognosis ($P = 0.0003$). High CD110 expression was an independent predictor of liver metastasis ($P = 0.0422$). Knockdown of CD110 expression significantly attenuated cell migration and invasion. Treatment with thrombopoietin promoted pancreatic cancer cell extravasation. In the presence of thrombopoietin, CD110 increased cell viability through the activation of the ERK–MYC signaling pathway. Knockdown of CD110 expression inhibited liver metastases in the mouse model.

Conclusions CD110 promotes pancreatic cancer progression and it may serve as a predictive factor for liver metastasis.

Keywords Pancreatic cancer · CD110 · TPO · Liver metastasis · Transendothelial migration

Introduction

Pancreatic ductal adenocarcinoma (PDAC) is the 4th most common cause of cancer-related death worldwide, with a 5-year survival rate of 5% (Stewart et al. 2014). The overwhelming majority of pancreatic cancer patients are diagnosed with liver metastasis (Hess et al. 2006) and liver metastasis is the leading cause of death with a 5-year survival rate of 2.7% for these patients (Noone et al. 2017). In the last decade, the median survival time of pancreatic cancer patients with liver metastases was less than 6 months (Hess et al. 2006). Curative resection becomes impossible once pancreatic cancer patients develop liver metastases (Gleisner et al. 2007). Therefore, the development of novel therapeutic strategies and/or biomarkers for liver metastasis is urgently needed for pancreatic cancer patients.

Tumor metastasis involves multistage processes including cancer cell local invasion, intravasation, survival in the circulation, extravasation, and colonization in secondary organs (Steeg 2006; Talmadge and Fidler 2010). Within the tumor

Electronic supplementary material The online version of this article (https://doi.org/10.1007/s00432-019-02860-z) contains supplementary material, which is available to authorized users.

✉ Kenoki Ohuchida
kenoki@surg1.med.kyushu-u.ac.jp

1 Department of Surgery and Oncology, Graduate School of Medical Sciences, Kyushu University, 3-1-1 Maidashi, Fukuoka 812-8582, Japan

2 Department of Advanced Medical Initiatives, Graduate School of Medical Sciences, Kyushu University, Fukuoka, Japan

3 Department of General Surgery, Shenzhen University General Hospital, Shenzhen, China

4 Department of Anatomical Pathology, Graduate School of Medical Sciences, Kyushu University, Fukuoka, Japan

5 Cancer Center, Kyushu University Hospital, Fukuoka, Japan

microenvironment, tumor-stromal interactions promote tumor local invasion and metastasis (Goetz et al. 2011; Sato et al. 2004). Epithelial–mesenchymal transition is also associated with pancreatic cancer cell invasiveness (Roy et al. 2011). Several proteins, such as transforming growth factor-β (TGFβ), vascular endothelial growth factor (VEGF) and matrix metalloproteinase-17 (MMP17), were reported to promote cancer cell intravasation through their activities (Anderberg et al. 2013; Chabottaux et al. 2009). CDC42, CCL2 and SPARC also have important roles in cancer cell extravasation leading to the promotion of metastasis (Qian et al. 2011; Reymond et al. 2012; Tichet et al. 2015). The results of these studies indicate that the genes involved in hematogenous metastasis could become therapeutic targets for advanced cancer.

CD110, also known as myeloproliferative leukemia protein (MPL), is a receptor for thrombopoietin (TPO) that plays an important role in megakaryocyte and platelet formation (Kaushansky 2006; Lok et al. 1994). Interactions between TPO and CD110 have been reported in leukemia and bone marrow diseases (Pikman et al. 2006; Yamazaki et al. 2009). In myeloproliferative neoplasms, CD110 mediates TPO-induced phosphorylation of ERK1/2 as well as induction c-MYC (Dorsch et al. 1997). Recently, aberrant expression of CD110 has been observed in several types of cancer. CD110 was also reported as an organ-specific marker of liver metastasis in colorectal cancer (Gao et al. 2013; Neyaz et al. 2018). Furthermore, previous report establishes a critical role of TPO-CD110 for colorectal cancer metastatic to the liver. Upon binding with TPO, CD110 regulates metabolic genes and promotes self-renewal of colorectal cancer cells (Wu et al. 2015). Thus, these data suggest that CD110 is a critical oncogenic protein and that CD110 facilitates liver metastases in cancer. However, the expression and function of CD110 in pancreatic cancer remain unknown.

Here, we investigated CD110 expression in PDAC tissue samples and cultured PDAC cells. We detected CD110 protein expression in pancreatic cancer cells and a significant involvement of CD110 in the migratory and invasive capacity of pancreatic cancer cells. TPO enhanced cancer cell extravasation and accelerated pancreatic cancer cell proliferation via activation of the ERK1/2-MYC signaling pathway. In vivo experiments revealed that knockdown of CD110 expression inhibited cancer cell extravasation and liver metastases. These data suggest that CD110 is a promising target in the treatment for the advanced pancreatic cancer.

Materials and methods

Pancreatic tissues and liver metastasis tissues

Pancreatic cancer and liver metastasis specimens were obtained from 86 patients who underwent pancreatectomy for pancreatic cancer at our institution from 1996 to 2011. Tissues were embedded, sliced and stained, and sections were observed using an optical microscope (BZ-X710; Keyence, Osaka, Japan). We also obtained normal pancreatic tissue samples for use as controls from intact pancreases resected for bile duct cancer. The clinicopathological characteristics of all patients are summarized in Supplementary Table S1.

Cell lines, culture conditions and treatment

The following pancreatic cancer cell lines were used in this study: AsPC-1, Hs766T, H48N, Capan-1, Capan-2 (American Type Culture Collection, Manassas, VA, USA), Panc-1 (Riken BioResource Center, Ibaraki, Japan); SUIT-2 (Japan Health Science Research Resources Bank, Osaka, Japan); BxPC-3 (National Kyushu Cancer Center, Fukuoka, Japan); and KP-3 (Dr H. Iguchi, National Shikoku Cancer Center, Matsuyama, Japan). All cell lines were maintained in DMEM (Sigma Chemical Co., St. Louis, MO, USA) supplemented with 10% FBS at 37 °C with humidified 90% air and 10% CO_2. Human pancreatic ductal epithelial (HPDE) cells were obtained from Dr. M.-S. Tsao (University of Toronto, Canada) and maintained in HuMedia-KG2 medium (KK-2150S KURABO, Osaka, Japan). HUVECs were obtained from Lonza (C2517A, Walkersville, MD, USA) and maintained in EBM-2 medium (Lonza). For treatment with TPO (T1568 Sigma–Aldrich, St. Louis, MO, USA), cells (2×10^5 cells/well in 6-well culture plates) were incubated with or without 10 ng/mL TPO in DMEM with 2% FBS for 30 min to 1 h before subsequent analyses.

Quantitative RT-PCR (qRT-PCR)

Total RNA was extracted from cultured cells using a High Pure RNA Isolation Kit (Roche Diagnostics, Mannheim, Germany) and DNase I (Roche Diagnostics, Sigma-Aldrich) treatment according to the manufacturer's instructions. qRT-PCR was performed using a QuantiTect SYBR Green Reverse Transcription-PCR kit (Qiagen, Tokyo, Japan) and a CFX96 Touch Real-Time PCR Detection System (Bio-Rad Laboratories, Hercules, CA, USA). We designed several specific primer sequences that were purchased from Sigma-Aldrich (Tokyo, Japan). Primer sequences are listed in Supplementary Table S2. mRNA expression levels are presented as relative expression normalized to 18S rRNA levels.

Western blot analysis

Western blotting was performed as previously described (Zheng et al. 2016). Cells were lysed in PRO-PREP (iNtRON Biotechnology, Seongnam, Korea) and proteins were separated on 4–15% Mini-PROTEAN TGX Precast

Gels (Bio-Rad Laboratories) and transferred to Trans-Blot Turbo Mini PVDF Transfer Packs (Bio-Rad Laboratories) using a Trans-Blot Turbo Transfer Starter System (Bio-Rad Laboratories). Membranes were incubated overnight at 4–8 °C with anti-CD110 (ab109003, Abcam, Cambridge, MA, USA), anti-TPO (ab196026, Abcam), anti-ERK1/2 (#4695, Cell Signaling Technology, Danvers, MA, USA), anti-phospho-ERK1/2 (#4370, Cell Signaling Technology), anti-c-MYC (#5605, Cell Signaling Technology), anti-phospho-c-MYC (#13,748, Cell Signaling Technology) or anti-β-actin (ab8227; Abcam). Membranes were then probed with appropriate secondary antibodies (Cell Signaling Technology). Immunoblot signals were detected by enhanced chemiluminescence with ChemiDoc XRS (Bio-Rad Laboratories).

Immunohistochemistry and evaluation

Tissues were sliced to sections of 4 mm. Endogenous peroxidase activity was blocked with methanol containing 0.3% hydrogen peroxidase. Antigen retrieval was performed by boiling in a microwave oven (citrate buffer, pH 6.0), as described before (Zheng et al. 2016). Sections were incubated with antibody targeting CD110, rabbit anti-TPOR (1:2000, #06-944; Anti-TPOR/c-Mpl Antibody, Millipore, Temecula, CA, USA) overnight at 4 °C and stained with EnVisionþ System-HRP Labeled Polymer Anti-Rabbit (#K4003; Dako, Glostrup, Denmark). Since there were no notable differences in CD110 staining intensity, we evaluated the ratio of CD110-positive pancreatic cancer cells. We counted the number of CD110-positive cells among pancreatic cancer cells in at least 5 fields per section at 200× magnification. Samples were divided into CD110-positive and CD110-negative groups; CD110-positivity was determined when the percent of CD110-positive pancreatic cancer cells was greater than 5%. We investigated the correlation with CD110-positivity with survival time, disease-free survival, liver metastases-free survival and clinicopathologic factors.

Silencing of CD110 using small interfering RNAs (siRNAs)

Gene silencing was achieved using small interfering RNA (siRNA, Qiagen) as described previously (Moriyama et al. 2010). The following siRNAs directed against human CD110 were used in the study: siRNA-1 (sense′, 5-GCG AUCUCGCUACCGUUUATT-3′; antisense, 5′-UAAACG GUAGCGAGAUCGCGG-3′); and siRNA-2 (sense, 5′-GAG GAUUGAGAUAAUCUAATT- 3′; antisense, 5′-UUAGAU UAUCUCAAU CCUCGT-3′). Qiagen all-star siRNA served as a negative control. Cells were transfected with siRNA by electroporation using a Nucleofector system (Amaxa Biosystems, Koln, Germany) according to the manufacturer's instructions.

Matrigel invasion and migration assays

The invasiveness and migration capacity of cancer cells was assessed by determining the number of cells invading or migrating across transwell chambers as previously described (Chijiiwa et al. 2016). For invasion assays, cells (1×10^5 cells/250 µl) were seeded in the upper transwell chamber (8 mm pore size; Becton Dickinson, Franklin Lakes, NJ, USA) containing 100 mL of reconstituted matrigel-coated membrane (20 mg/well, BD Biosciences, Bedford, MA, USA) at 24 h after knockdown of CD110. Cells were incubated for 48 h and the number of invaded cancer cells was counted. Cell migration assays were performed using the same protocol as the invasion assay without a matrigel-coated membrane. Cells were allowed to migrate and counted 24 h after cell seeding into the upper chamber. In both assays and at each time point, invaded or migrated cells at the bottom of the chamber were fixed with 70% ethanol and stained with hematoxylin and eosin, and five random fields were counted at 100× magnification (BZ-X710; Keyence). Each experiment was performed in triplicate and repeated at least three times.

Cell viability assay

Cells (1×10^3 cells/well) were seeded in 96-well plates (Greiner Bio-One, Frickenhausen, Germany) at 48 h after transfection with siRNA. Cell viability examined using the CellTiter-Glo Luminescent Cell Viability Assay Kit (G7570, Promega, Madison, WI, USA) following the manufacturer's instructions. For TPO treatment, cells (1.5×10^3 cells/well) were incubated with or without TPO in 2% FBS/DMEM in 96-well culture plates. Background was subtracted using values from wells containing only culture medium.

Transendothelial migration assays

A total 1×10^5 red fluorescence protein (RFP; OHS5833 Dharmacon, Lafayette, CO, USA)-transfected HUVECs were plated in the upper chamber of a gelatin-coated transwell insert and grown in complete endothelial medium to confluence. AsPC-1cells transfected with siRNA targeting CD110 or control siRNA were pulsed with 5 µM CellTracker Green CMFDA dye for 30 min, detached by HyQTase treatment (HyClone, Marlborough, MA, USA) and plated on top of the endothelial monolayer. 10 ng/ml TPO containing EGM2 medium was used as a chemoattractant in the bottom chamber. Cells were allowed to migrate for 7–24 h at 37 °C in 10% CO_2. Cells on the apical side of each insert were scraped off, and cells that migrated to the basolateral side of the membrane were visualized with an immunofluorescent microscope at 100× magnification (BZ-X710; Keyence). Pictures of five random fields were captured for

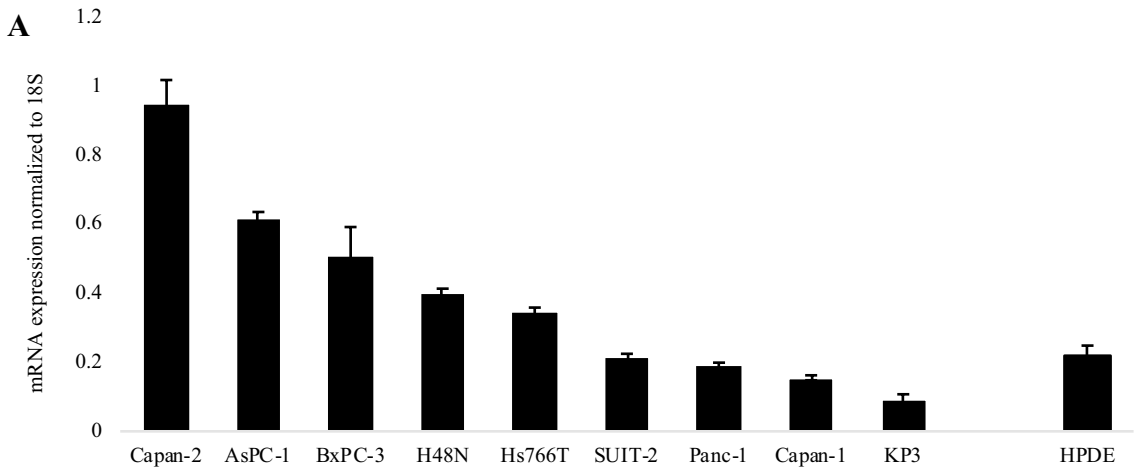
A
1.2
1
0.8
0.6
0.4
0.2
0
mRNA expression normalized to 18S
Capan-2
AsPC-1
BxPC-3
H48N
Hs766T
SUIT-2
Panc-1
Capan-1
KP3
HPDE

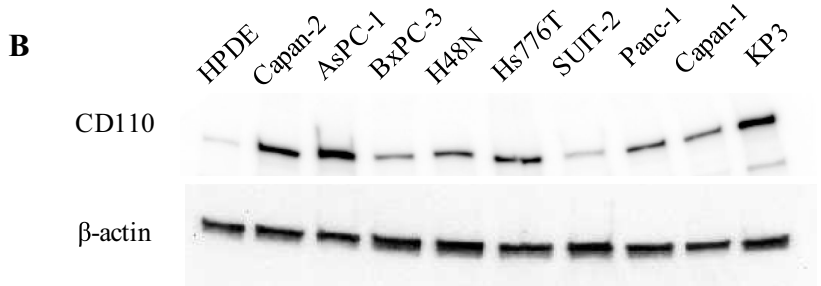
B
HPDE
Capan-2
AsPC-1
BxPC-3
H48N
Hs776T
SUIT-2
Panc-1
Capan-1
KP3
CD110
β-actin

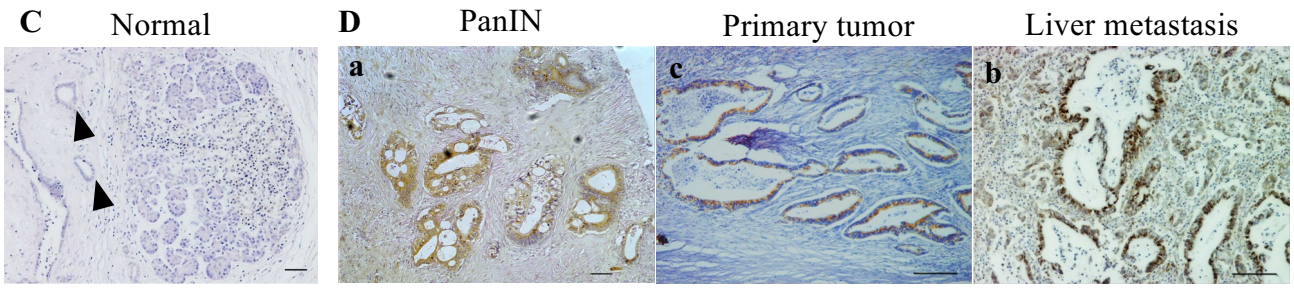
C
Normal
D
PanIN
Primary tumor
Liver metastasis
a
c
b

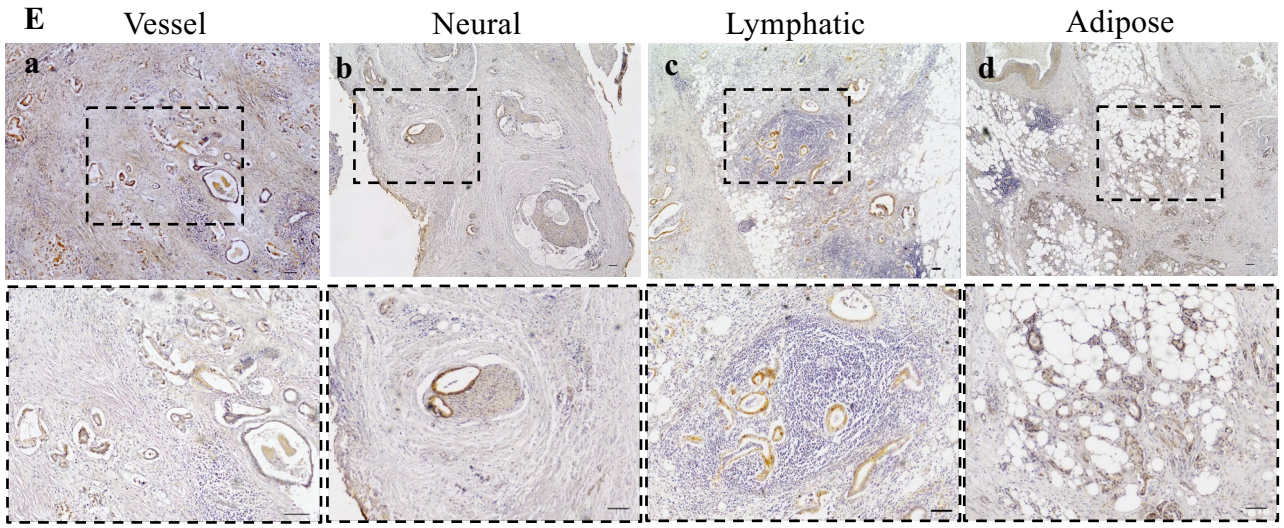
E
Vessel
Neural
Lymphatic
Adipose
a
b
c
d

◂**Fig. 1** CD110 expression in pancreatic cancer. **a** CD110 mRNA expression levels in pancreatic cancer cell lines and human normal pancreatic epithelial (HPDE) cells. CD110 mRNA expression was normalized by 18S expression. **b** CD110 protein expression level in pancreatic cancer cell lines and HPDE cells. **c** CD110 expression was undetectable in normal duct (arrowhead). **d** CD110 expression was detected in PanIN tissue (**a**), primary tumor (**b**), and liver metastases (c). **e** CD110 expression was detected in tissues with of vessel invasion (**a**), neural invasion (**b**), lymphatic invasion (**c**) and adipose invasion (**d**). Bottom row shows images at magnification 100×. Scale bars = 100 μm

quantification. All the experiments were performed in triplicate and repeated at least three times.

Microarray

Total RNA was isolated from cultured cells using a High Pure RNA Isolation Kit with DNase digestion (Roche Diagnostics, Mannheim, Germany). RNA quality was evaluated using the Agilent 2200 TapeStation system (Agilent Technologies, CA, USA) for microarray analysis. RNA was labeled and hybridized to the Agilent SurePrint G3 Human Gene Expression Microarray 8 × 60K Ver.3.0 (Agilent Technologies). Data were analyzed using Feature Extraction software (Agilent Technologies). Compute overlaps investigation of gene set using Molecular Signatures database (Gene Set Enrichment Analysis).

Establishment of AsPC-1 small hairpin RNA- and luciferase-expressing cells

Two CD110 small-hairpin (shRNA) vectors (#TRCN9195/9020; Sigma-Aldrich) and a firefly luciferase expression vector (#LVP326; GenTarget, San Diego, CA, USA) were transfected into AsPC-1 cells according to the manufacturer's instructions. Non-targeting shRNA (SHC016V, Sigma Aldrich) was used as control. Puromycin (#631,305; Takara, Shiga, Japan) was used to select CD110 or control shRNA-stably expressing clones, and blasticidin S hydrochloride (#15,205; Sigma-Aldrich) was used to select luciferase-expressing clones; selection was performed for more than 3 weeks. shRNA-mediated CD110 knockdown was confirmed by quantitative RT-PCR and Western blotting.

In vivo experiments

BALB/c AJcl nu/nu female mice were purchased from Clea (Tokyo, Japan) and transported to our institution at 4 weeks old. 10 Mice were randomized divided into two groups. After 1 week of accustomization, luciferase-expressing AsPC-1 cells were resuspended in 100 μl of PBS and injected into the spleen of nude mice. Luciferase activity of liver metastasis was monitored and quantified using the IVIS Spectrum. (Caliper Life Sciences, Waltham, MA, USA), after injecting 150 mg D-luciferin (#LK10000; Oz Biosciences, Marseille, France) into the intraperitoneal cavity of anesthetized mice. In the short-term liver colonization assay, 1×10^6 luciferase-expressing siRNA-transfected AsPC-1 cells were injected into the spleen of nude mice and luciferase activities of mice livers were observed after 24 h of implantation. In the experimental liver metastasis assay, 1×10^6 luciferase- and shRNA-stably expressing AsPC-1 cells were injected into the spleen of nude mice and liver metastasis was monitored and quantified every week. Luciferin emission was measured on the following day as a standard, and emission was quantified using Living Image software, version 4.4 (Summit Pharmaceuticals International Corporation, Tokyo, Japan), until mice were sacrificed.

Statistical analysis

The x2-test was used to assess correlations between CD110 expression and clinicopathological characteristics. Survival analysis was performed using Kaplan–Meier analysis and curves were compared using the log-rank test. For in vitro experiments, values are expressed as the mean ± standard deviation. Comparisons between two groups were made using the Student's *t* test. Statistical significance was defined as $P < 0.05$. All statistical analyses were performed using JMP 11.0.0 software (SAS Institute, Cary, NC, USA).

Results

Elevated CD110 expression in pancreatic cancer cell lines, primary tumors and liver metastases

First, we investigated CD110 expression in HPDE cells and pancreatic cancer cell lines. The qRT-PCR and western blotting results showed that CD110 gene and protein expressions were slightly detectable in HPDE cells (Fig. 1a, b). The pancreatic cancer cell lines expressed CD110 mRNA and protein at variable levels. We further examined CD110 expression using resected human tissues of normal pancreas and primary tumors and liver metastases from pancreatic cancer cases. CD110 expression was not detectable in normal pancreatic ducts (Fig. 1c). However, CD110 expression was observed in PanIN tissues, the primary tumor and liver metastases (Fig. 1d). Furthermore, we found that CD110-positive cancer cells were especially located in lesions with vessel invasion, neural invasion, lymphatic invasion, and adipose invasion (Fig. 1e).

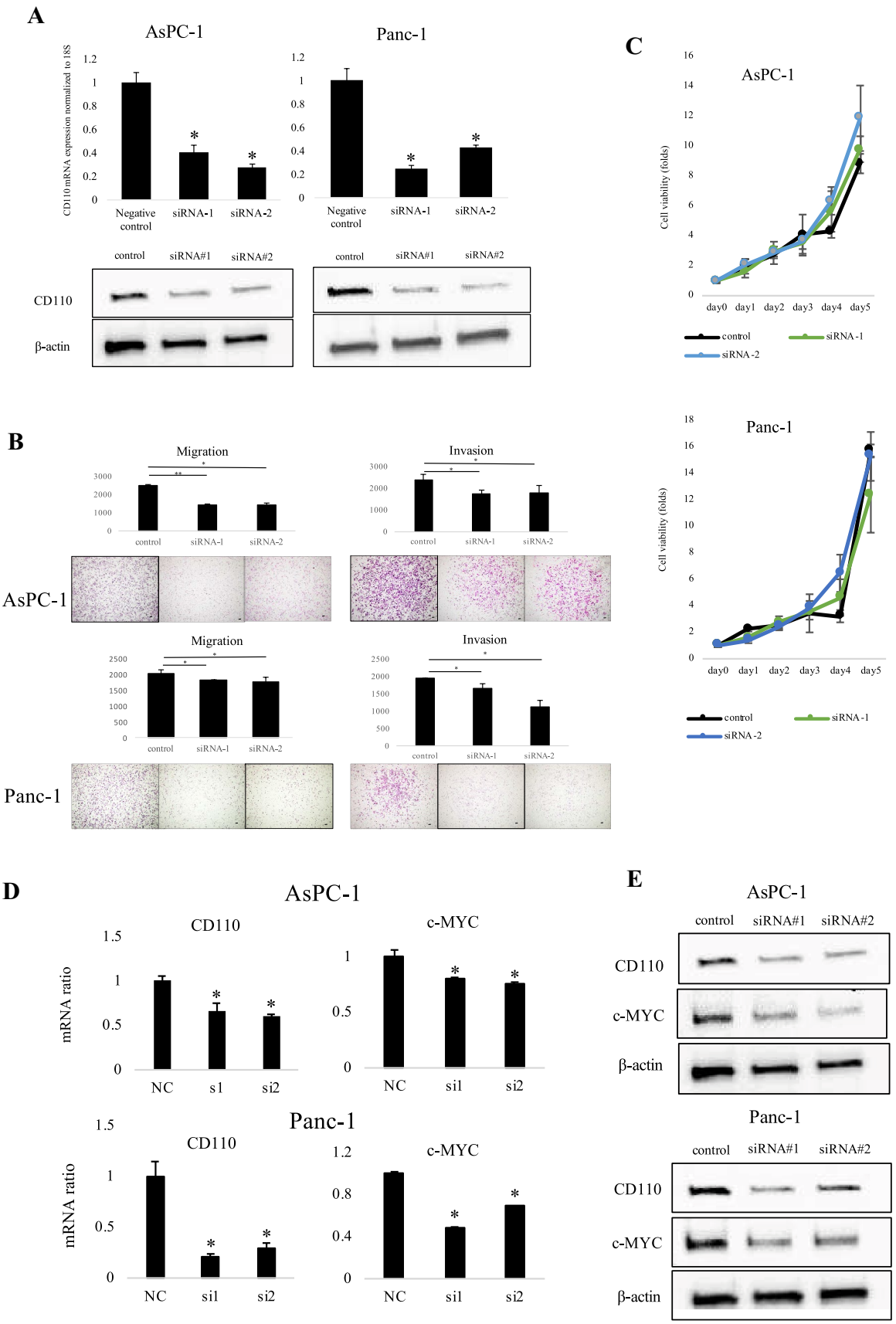
A
AsPC-1
Panc-1
CD110 mRNA expression normalized to 18S
Negative control
siRNA-1
siRNA-2
control
siRNA#1
siRNA#2
CD110
β-actin
B
Migration
Invasion
AsPC-1
Panc-1
C
AsPC-1
Panc-1
Cell viability (folds)
day0 day1 day2 day3 day4 day5
control
siRNA-1
siRNA-2
D
AsPC-1
Panc-1
CD110
c-MYC
mRNA ratio
NC
s1
si1
si2
E
AsPC-1
Panc-1
CD110
c-MYC
β-actin

◂**Fig. 2** Knockdown of CD110 reduces migration and invasion but not proliferation of pancreatic cancer cells. **a** qRT-PCR (top) and western blot (bottom) of CD110 mRNA and protein levels in cells transfected with siRNAs targeting CD110 or negative control. $*P<0.05$. **b** Cells were transfected with the indicated siRNAs for 48 h and migration and invasion assays were performed for 48 and 24 h. Graphs show the quantification of cells calculated from five fields. Original magnification: 40×. Scale bars = 100 µm. $*P<0.05$, $**P<0.01$. **c** Cell viability of cancer cells as determined by CellTiter-Glo luminescent cell viability assay with CD110 knockdown. **d** qRT-PCR and **e** western blotting showed that mRNA and protein expression of c-MYC was decreased by CD110 knockdown. $*P<0.05$, $**P<0.01$

The functional role of CD110 in PDAC cells in vitro

To examine the functional role of CD110 in cancer cells, we investigated the effect of CD110 knockdown on the invasiveness and migration activities of pancreatic cancer cell lines using a transwell system. Knockdown of CD110 expression on AsPC-1 and PANC-1 cancer cells were achieved stably and efficiently using siRNA (Fig. 2a). Both the migration and invasion activities of cancer cells were significantly decreased after CD110 knockdown compared with control cells (Fig. 2b). However, proliferation was not significantly changed after CD110 knockdown (Fig. 2c).

A previous study indicated that CD110 was involved in regulating its downstream targets, the transcriptional oncoprotein c-MYC (Besancenot et al. 2010; Chanprasert et al. 2006). Thus, we investigated both mRNA and protein levels of c-MYC in cells with CD110 knockdown and found that both gene and protein c-MYC expressions were downregulated in both cancer cell lines (Fig. 2d, e).

CD110 promotes cancer cell transendothelial migration and extravasation

Previous studies described a link between CD110 and distant liver metastases, (Gao et al. 2013) especially in the presence of its ligand TPO (Wu et al. 2015). TPO is primarily produced in both parenchymal cells and sinusoidal endothelial cells of the liver (Bartley et al. 1994; Hitchcock and Kaushansky 2014). We investigated TPO expression in pancreatic tissues and cell lines and found that TPO was undetectable in the majority of pancreatic cancer cell lines and in pancreatic cancer tissues (Fig. 3a, b). As shown in previous reports, TPO was specifically highly expressed in the liver of pancreatic cancer patients (Bartley et al. 1994; Hitchcock and Kaushansky 2014).

Crossing the endothelial barrier is an important step for the metastasis of cancer cells. Based on the number of studies on the TPO-CD110 interaction,(Besancenot et al. 2014; Dong-Feng et al. 2014; Wu et al. 2015) we hypothesized that TPO serves as a chemoattractant cytokine that induces CD110-positive cancer cells to cross the endothelial barrier towards TPO-expressing sites in the liver. To examine the potential role of TPO-CD110 signaling in cancer cell extravasation, we performed a transendothelial migration assay using a modified Boyden chamber model, as reported previously (Qian et al. 2011; Reymond et al. 2012; Tichet et al. 2015). The transendothelial migration assay is used to evaluate cell ability to migrate through endothelial cell monolayer, which is involved in the extravasation (Reymond et al. 2013). Knockdown of CD110 expression alone did not alter the transendothelial migration of pancreatic cancer cells. However, while treatment with TPO increased transendothelial migration, knockdown of CD110 significantly inhibited TPO-induced migration of PDAC cells (Fig. 3c).

TPO-mediated induction of proliferation and ERK/MYC signaling involves CD110

We next examined other effects of TPO on cancer cells with or without CD110 expression. TPO treatment alone had no impact on the expression of CD110 in PDAC cells (data not shown). TPO did not impact the invasion and migration abilities of cancer cells that harbored CD110 expression (data not shown) but enhanced the proliferation of these cells in a dose-dependent manner (Fig. 3d). We next used CD110 knockdown cancer cells to investigate whether this effect was mediated by its interaction with CD110 and found that knockdown of CD110 attenuated the proliferation enhanced by TPO (Fig. 3e), suggesting that TPO stimulated proliferation via its interaction with CD110. Since several reports indicated TPO-CD110 regulate phospho-ERK1/2 expression (Pikman et al. 2006; Rojnuckarin et al. 1999; Rouyez et al. 1997). We also found that the protein expression levels of phospho-ERK1/2 and phospho-c-MYC were upregulated after TPO treatment only in cells expressing CD110 and not in CD110 knockdown cells (Fig. 3f).

Knockdown of CD110 decreased early liver metastasis of PDAC cells

To investigate the functional role of CD110 on cancer cell extravasation in vivo mouse model, we performed early liver metastasis assays to monitor cancer cell extravasation and colonization activities. Mouse TPO could interact with human CD110 as described (Gao et al. 2013). Luciferase-expressing AsPC-1 cells stably expressing control siRNA or CD110 siRNA were transplanted into nude mice using intrasplenic injection and evaluated 24 h later (Fig. 4a). Mice injected with AsPC-1 cells with CD110 knockdown showed significantly decreased early liver metastasis (Fig. 4b, c). Moreover, histological analysis using luciferase staining revealed that cancer cell extravasation into liver parenchyma was suppressed in animals injected with CD110 knockdown cells (Fig. 4d), indicating that knockdown of CD110 expression in AsPC-1 cells decreased extravasation ability. To

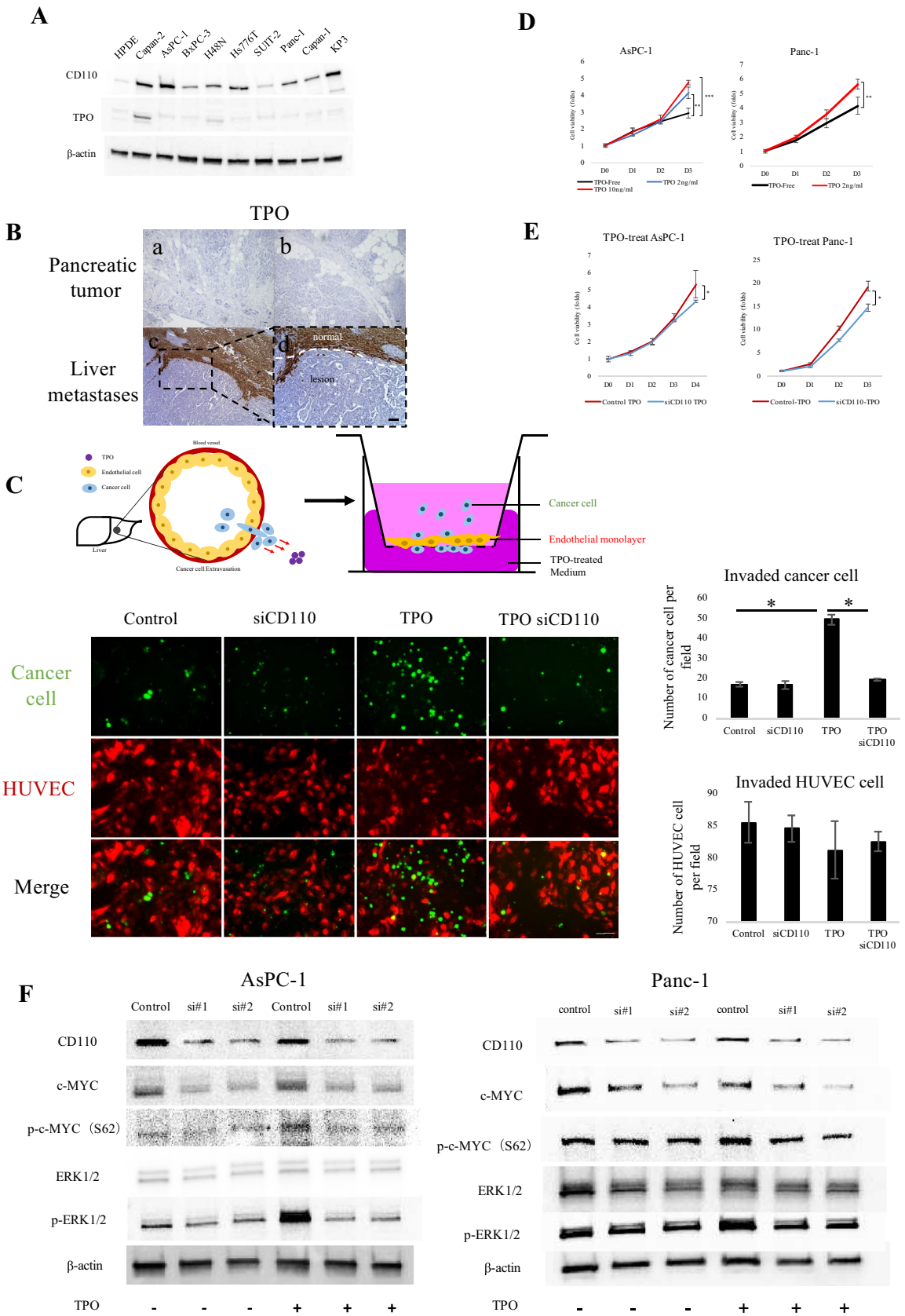
A
HPDE
Capan-2
AsPC-1
BxPC-3
H48N
Hs776T
SUIT-2
Panc-1
Capan-1
KP3
CD110
TPO
β-actin
D
AsPC-1
Panc-1
Cell viability (folds)
D0 D1 D2 D3
TPO-Free
TPO 10ng/ml
TPO 2ng/ml
B
TPO
Pancreatic tumor
Liver metastases
a
b
c
d
normal
lesion
E
TPO-treat AsPC-1
TPO-treat Panc-1
D0 D1 D2 D3 D4
Control TPO
siCD110 TPO
Control-TPO
siCD110-TPO
C
Blood vessel
TPO
Endothelial cell
Cancer cell
Liver
Cancer cell Extravasation
Cancer cell
Endothelial monolayer
TPO-treated Medium
Control
siCD110
TPO
TPO siCD110
Cancer cell
HUVEC
Merge
Invaded cancer cell
Number of cancer cell per field
Control
siCD110
TPO
TPO siCD110
Invaded HUVEC cell
Number of HUVEC cell per field
F
AsPC-1
Panc-1
Control
si#1
si#2
control
CD110
c-MYC
p-c-MYC（S62）
ERK1/2
p-ERK1/2
β-actin
TPO

◂**Fig. 3** Functional role of the CD110-TPO axis in transendothelial migration of pancreatic cancer cells. **a** TPO protein expression was undetectable in the majority of pancreatic cancer cell lines and HPDE cells. **b** TPO expression was undetectable in pancreatic cancer tissues (**a**) and (**b**). TPO expression was detected in liver metastatic tissues (**c, d**). Normal tissue and metastasis lesion were indicated. Scale bars = 100 μm. **c** TPO-containing medium increased pancreatic cancer cell extravasation in transendothelial migration assays. AsPC-1 cells were transfected with control or CD110 siRNA (and then dye with Cell Tracker green) and incubated in the top chamber containing HUVEC monolayer for 24 h; the bottom chamber contained control or 10 ng/ml TPO-containing medium. Quantification of five fields of extravasation cells is shown on the right. Scale bars = 100 μm. $^{*}P < 0.05$. **d** TPO increased the proliferation of pancreatic cancer cells in a dose-dependent manner. $^{*}P < 0.05$, $^{**}P < 0.01$, $^{***}P < 0.001$. **e** Proliferation enhancement by TPO was attenuated by CD110 knockdown. $^{*}P < 0.05$. **f** Western blot analysis of ERK, p-ERK, MYC and p-MYC levels in pancreatic cancer cells transfected with CD110 siRNA and treated with 10 ng/ml TPO for 30 min

investigate the effects of CD110 knockdown on the molecular mechanism in PDAC cells with presence of TPO stimulation, microarray was carried out using AsPC-1 cells with CD110-intact or CD110-knockdown under stimulation of TPO. A heatmap of RNA profiles showed 632 genes were identified as genes commonly changed in CD110- knockdown AsPC-1 cells under TPO stimulation (Fig. 4e and Fig. S1). Moreover, Compute overlaps analysis using Molecular Signatures database (Liberzon et al. 2015; Subramanian et al. 2005) revealed that these genes were actively involved in a cytokine–cytokine receptor interaction and leukocyte transendothelial migration KEGG pathway (Fig. 4f and Fig. S2).

Knockdown CD110 inhibited long-term liver metastasis *in vivo*

We next investigated the long-term effects of CD110 knockdown on liver metastasis in the mouse model. Luciferase-expressing AsPC-1 cells transfected with control shRNA or CD110 shRNA were transplanted into nude mice using intrasplenic injection as before and evaluated every week for 28 days (Fig. 5a–c). Consistent with results from the early liver metastasis assay, liver metastases from mice injected with shCD110-expressing cells showed significantly reduced luciferase activities ex vivo compared with controls and fewer numbers of metastases (Fig. 5d, e). Compared with the control group, mice with shCD110 cells exhibited decreased liver weight and volume, but the differences were not significant (data not shown). TPO expression was detectable in almost all of normal hepatic cell in mouse liver. Especially, TPO was extremely expressed at the boundary of liver metastasis lesions. In addition, we found that p-ERK1/2, Ki67 and TPO expression were reduced in pancreatic cancer cells of liver metastatic lesions (Fig. 5f). Taken together, these results indicate that knockdown of CD110 reduced colonization and proliferation of pancreatic cancer cells and inhibited liver metastasis formation in vivo.

Correlations between CD110 expression and clinicopathological characteristics

We next investigated CD110 expression in resected samples from 86 patients with pancreatic cancer using immunohistochemical analysis and evaluated the correlation of CD110 expression with clinicopathological factors. We divided the pancreatic cancer patients into two groups: CD110-positive group (CD110 + cancer cells ≥ 5%; $n = 49$, Fig. 6a) and CD110-negative group (CD110 + cancer cells < 5%; $n = 37$, Fig. 6b). Patients in the CD110-positive group had more frequent residual tumor status ($P = 0.0115$), advanced pT, pN and UICC stage ($P = 0.0019$, $P = 0.0021$, $P = 0.0137$, respectively), higher vessel invasion ($P < 0.0082$) and lymphatic invasion ($P = 0.0320$) than patients in the CD110-negative group (Table 1).

Prognostic significance of CD110 expression in pancreatic cancer cells

We then investigated the association between CD110 expression and overall survival and disease-free survival of the 86 pancreatic cancer patients with surgical resection. CD110-positive patients demonstrated worse survival than CD110-negative patients ($P = 0.0003$; Fig. 6c) and had a short duration disease-free time ($P < 0.0001$; Fig. 6d). The median survival was 18.7 months for the CD110-positive group and 68.0 months for the CD110-negative group, and 19 of the 43 CD110-negative patients (44.53%) survived more than 5 years following surgical resection (Table 2). Furthermore, univariate analysis revealed that positive CD110 expression ($P < 0.0003$), primary tumor invasion (pT, $P < 0.0332$), lymph node metastasis (pN, $P < 0.0236$), vascular invasion ($P = 0.0117$) and lymphatic invasion ($P = 0.0001$) were all associated with overall survival (Table 3). We next performed multivariate analysis based on the Cox proportional hazard model using all parameters that were significantly associated with survival by univariate analysis. Multivariate analysis showed significant independent prognostic values in CD110 positivity (relative risk 2.107; $P = 0.0130$) and positive lymphatic invasion (relative risk 2.799; $P = 0.0132$; Table 3).

Correlations between liver metastasis and clinicopathological characteristics

A previous study demonstrated that CD110 expression was correlated with liver metastasis in colorectal cancer patients, and our present in vitro data demonstrated an involvement

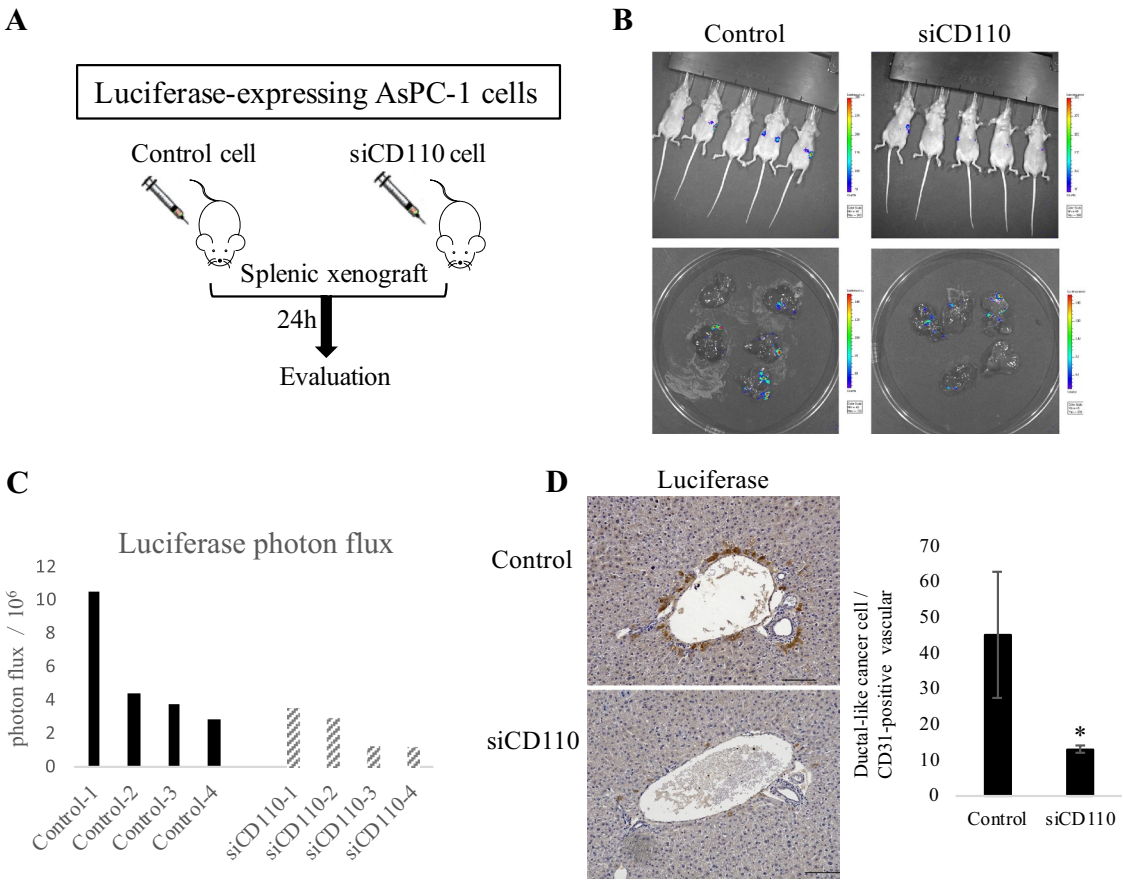

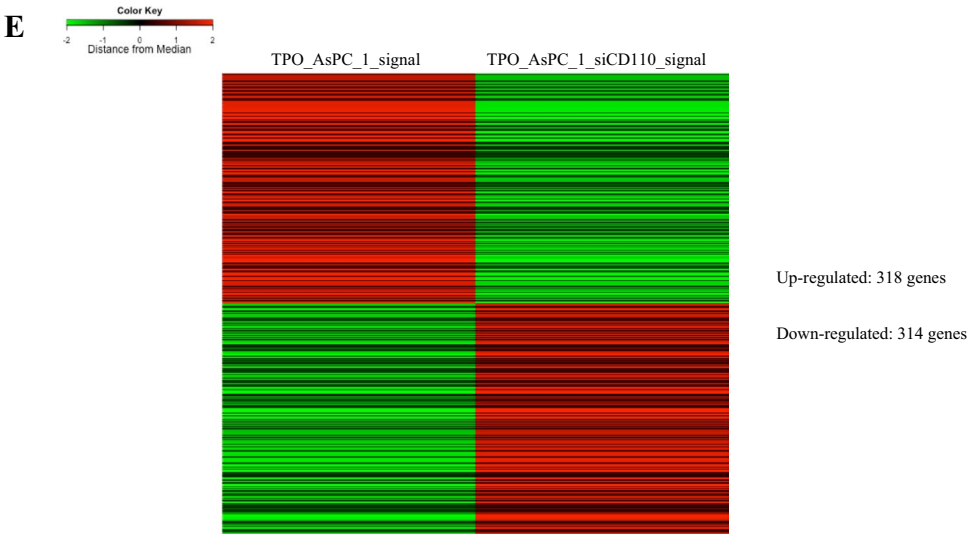

F

Gene Set Name	# Genes in Gene Set (K)	Description	# Genes in Overlap (k)	k/K	p-value	FDR q-value
KEGG_CYTOKINE_CYTOKINE_RECEPTOR_INTERACTION	267	Cytokine-cytokine receptor interaction	13	0.0487	7.75E-07	1.44E-04
KEGG_INTESTINAL_IMMUNE_NETWORK_FOR_IGA_PRODUCTION	48	Intestinal immune network for IgA production	5	0.1042	6.13E-05	5.70E-03
KEGG_HYPERTROPHIC_CARDIOMYOPATHY_HCM	85	Hypertrophic cardiomyopathy (HCM)	6	0.0706	1.03E-04	6.36E-03
KEGG_DILATED_CARDIOMYOPATHY	92	Dilated cardiomyopathy	6	0.0652	1.59E-04	7.39E-03
KEGG_LEUKOCYTE_TRANSENDOTHELIAL_MIGRATION	118	Leukocyte transendothelial migration	6	0.0508	6.08E-04	2.04E-02
KEGG_REGULATION_OF_ACTIN_CYTOSKELETON	216	Regulation of actin cytoskeleton	8	0.037	6.59E-04	2.04E-02
KEGG_NICOTINATE_AND_NICOTINAMIDE_METABOLISM	24	Nicotinate and nicotinamide metabolism	3	0.125	1.16E-03	3.07E-02
KEGG_CHEMOKINE_SIGNALING_PATHWAY	190	Chemokine signaling pathway	7	0.0368	1.46E-03	3.40E-02

◂**Fig. 4** Knockdown of CD110 reduced metastasis in a short-term liver metastasis assay. **a** Luciferase-expressing AsPC-1 tumor cells stably expressing control siRNA or CD110 siRNA were injected into the spleen of nude mice and after 24 h, livers were examined. **b** Imaging of mice after 24 h, description of the samples shown in the dishes in the bottom row. **c** Luciferase activity revealed decreased emission value in livers of siCD110 xenograft mice. **d** H&E and CD31 immunohistochemical staining revealed reduction of transendothelial migration of cancer cells in siCD110 xenograft mice. $*P<0.05$. **e** Microarray analysis compare with CD110-intact and CD110-knockdown AsPC-1 cells with presence of TPO stimulation. **f** Compute overlaps analysis indicated KEGG pathways involved in CD110 knockdown of AsPC-1 cells with TPO stimulation

of CD110 expression in liver metastasis in PDAC. Therefore, we investigated the correlation between liver metastasis frequency and clinicopathological factors including CD110 expression. Liver metastasis was correlated with CD110 positive expression ($P=0.0422$) and poorly differentiated histological grade ($P=0.0026$; Table 4). Multivariate analysis showed that CD110 positive expression ($P=0.0498$) and poorly differentiated histological grade ($P=0.0040$; Table 5) were independent factors to predict liver metastasis. CD110-positive expression was also correlated with a shorter time until liver metastasis relapse ($P<0.001$; Fig. 6e).

Discussion

In the present study, we investigated CD110 expression in pancreatic cancer cells and its functional impact on pancreatic cancer progression. Our results showed that CD110 was widely detected in pancreatic cancer cell lines and associated with the migratory and invasive capacity of cancer cells. Especially, The data suggest that the change in the expression of CD110 regulates the invasion and migration of pancreatic cancer cells without binding its ligand, TPO. CD110 exists as a mixture of monomers and dimers independent of TPO stimulation, and its overexpression induces its dimerization possibly leading to the activation of downstream signaling (Kaushansky 2005; Sakamoto et al. 2016). Therefore, knockdown of CD110 in the present study may inhibit its dimerization to attenuate cell migration and invasion although the further examination will be needed. CD110-TPO enhanced the capacity of cancer cell extravasation and accelerated pancreatic cancer cell proliferation, and these effects may involve the ERK1/2-MYC signaling pathway in vitro. In vivo experiments using a cancer cell splenic injection model revealed that knockdown of CD110 inhibited cancer cell extravasation and liver metastases. Moreover, immunohistochemical analyses showed CD110 expression was significantly correlated with vessel and lymphatic invasion. In addition, CD110 expression was a predictive marker of poor prognosis and relapse of liver metastasis. These data suggest that CD110 or CD110-TPO signaling may serve as promising candidates for biological markers or therapeutic targets of pancreatic cancer, especially for liver metastasis.

In the PDAC tumor tissues examined in our study, not all cancer cells were positive for CD110 expression, even in the same tumors derived from one patient. In both our in vitro and in vivo studies, only a few cancer cells were able to migrate and metastasize to liver. CD110 was reported to be a liver metastasis-specific factor in colorectal cancer. Such organ-specific metastasis is possibly dependent on chemokines in the secondary organ. Chemokines such as CXCL12 in distant organs can attract cancer cells that express its receptors, such as CXCR4 and CXCR7, stimulating prostate cancer and breast cancer cell transendothelial migration (Kukreja et al. 2005; Wendel et al. 2012; Zabel et al. 2009). Similarly, we demonstrated a functional role for the CD110-TPO axis in transendothelial migration, which may involve the activation of p-ERK in pancreatic cancer cells. In the present study, CD110-TPO signaling increased invasiveness and migration ability and the activation of ERK, which has been correlated with invasiveness and metastasis in several cancers (Choi and Helfman 2014; Principe et al. 2017). In myeloproliferative neoplasm, CD110 was reported to bind with calreticulin (Elf et al. 2016; Sangkhae et al. 2014) and promote the ERK signaling pathway (Sheng et al. 2017). Our findings demonstrated that CD110-TPO triggered p-ERK upregulation and promoted transendothelial migration without increasing cancer cell adhesion capacity during pancreatic cancer progression (data not shown). In breast and prostate cancer, CXCL12-CXCR4 and CXCL12-CXCR7 signaling increased cancer cell adhesion to ECM and/or HUVECs (Engl et al. 2006; Zabel et al. 2009) and promoted transendothelial migration. These data suggest that there are diverse mechanisms to induce transendothelial migration depending on the type of cancer.

The level of p-ERK expression is high in PDAC tissues compared with normal tissues (Principe et al. 2017). An inhibitor of p-ERK was reported to suppress the proliferation of human pancreatic cancer cells in vitro and tumor growth of xenograft model in vivo (Hayes et al. 2016; Morris et al. 2013). These data provide strong evidence for the significance of p-ERK inhibition in pancreatic cancer therapy strategies. Prolonged ERK phosphorylation stimulates c-MYC phosphorylation (Tsai et al. 2012; Wang et al. 2011). In contrast, inhibition of p-ERK is correlated to c-MYC degradation in Kras-mutant pancreatic cancer (Hayes et al. 2016). c-MYC is a proto-oncogene that acts as a downstream transcriptional effector of many signaling pathways and functions in cell growth control, differentiation and apoptosis (Palomero et al. 2006; Weng et al. 2006). A novel mouse model of inducible pancreatic-specific loss of c-MYC showed that c-MYC plays

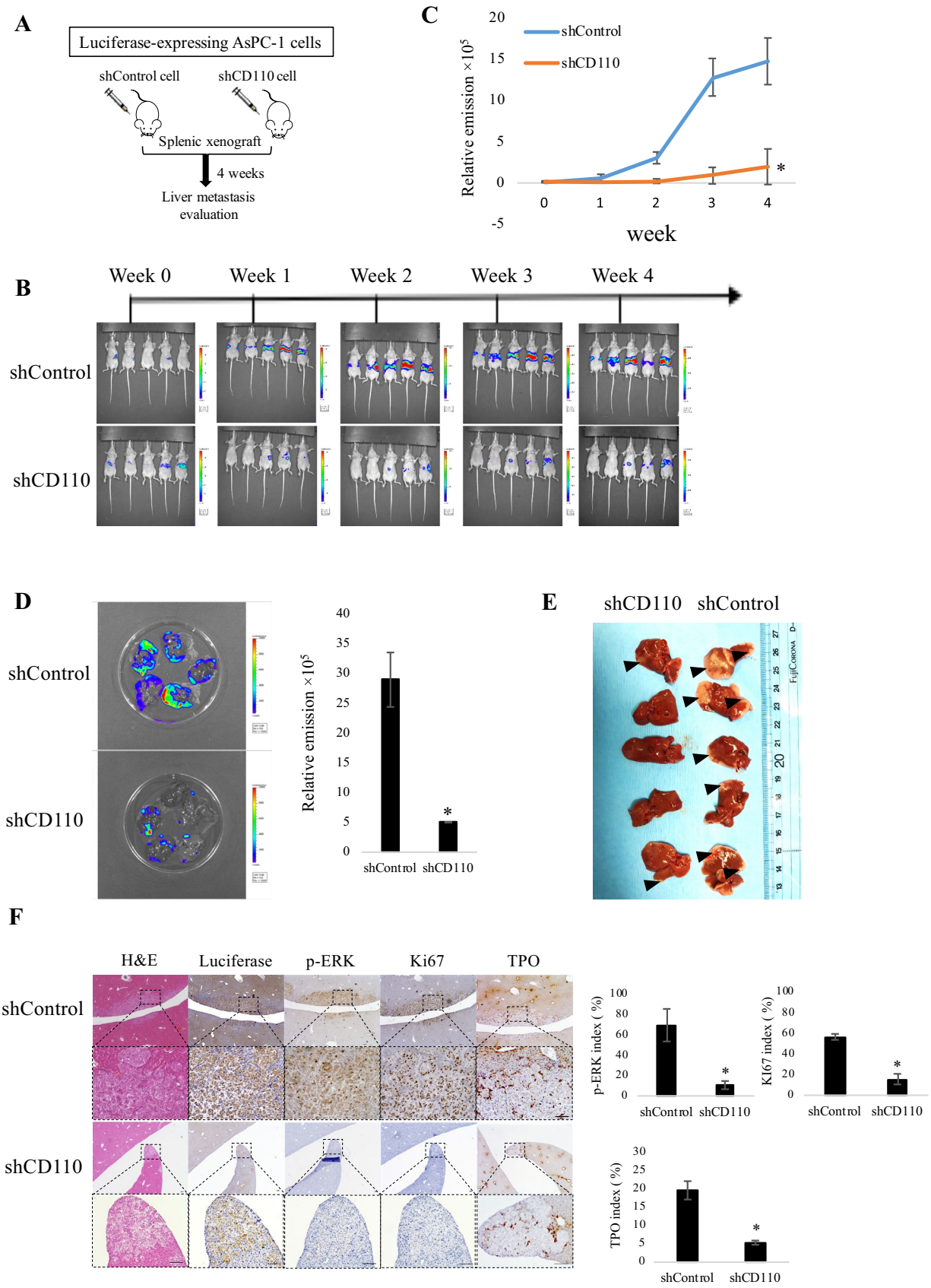
A
Luciferase-expressing AsPC-1 cells
shControl cell
shCD110 cell
Splenic xenograft
4 weeks
Liver metastasis evaluation
C
Relative emission ×10^5
shControl
shCD110
week
B
Week 0
Week 1
Week 2
Week 3
Week 4
shControl
shCD110
D
shControl
shCD110
Relative emission ×10^5
shControl shCD110
E
shCD110 shControl
F
H&E
Luciferase
p-ERK
Ki67
TPO
shControl
shCD110
p-ERK index (%)
KI67 index (%)
TPO index (%)
shControl shCD110

◂**Fig. 5** CD110 reduced metastasis in a long-term in vivo liver metastasis assay. **a** Luciferase-expressing AsPC-1 cells were transfected with CD110 shRNA and then injected into the spleen of nude mice. **b, c** Liver metastasis was monitored and quantified weekly for 4 weeks using bioluminescence imaging. Mice injected with cells expressing shCD110 showed significantly reduced liver metastasis as observed by decreased luciferase activity. $*P < 0.05$. **d** Ex vivo bioluminescence showed that knockdown of CD110 significantly reduced liver metastasis formation. $*P < 0.05$. **e** Gross pathology showed that knockdown of CD110 significantly reduced liver metastasis formation (arrowheads: metastasis lesions). **f** Immunohistochemical staining showed that p-ERK, Ki67 and TPO expression were decreased in xenografts from mice injected with CD110 knockdown cells with positive luciferase expression

a significant role in the initiation, progression, maintenance and recurrence of PDAC (Lin et al. 2013). c-MYC expression in colorectal cancer stem cells is significantly upregulated by TPO treatment (Wu et al. 2015). In the present study, knockdown of CD110 led to downregulation of c-MYC transcriptional levels and TPO-CD110 signaling led to c-MYC phosphorylation via ERK activation. The present data showed that TPO-CD110 signaling induced the phosphorylation of MYC-S62, which promotes the cell proliferation (Sears et al. 2000). On the other hand, accumulation of MYC-S62 phosphorylation reduces the transcriptional level of MYC (Wang et al. 2011) and the decreased transcriptional level of MYC inhibits PDAC cell invasion (Vaseva et al. 2018). Therefore, the phosphorylation of MYC-S62 induced by CD110 binding with TPO possibly controls the cell proliferation and cell invasion via the different mechanism, respectively.

In conclusion, positive CD110 expression in PDAC was associated with poor prognosis and liver metastasis of human PDAC samples. The TPO-CD110 axis promoted cancer cell extravasation via activation of the ERK-MYC pathway in vitro and in vivo. These data suggest that CD110 plays an important role in pancreatic cancer progression, especially in liver metastasis. Therefore, a new CD110-TPO targeting therapeutic strategy might improve the prognosis of patients with pancreatic cancer.

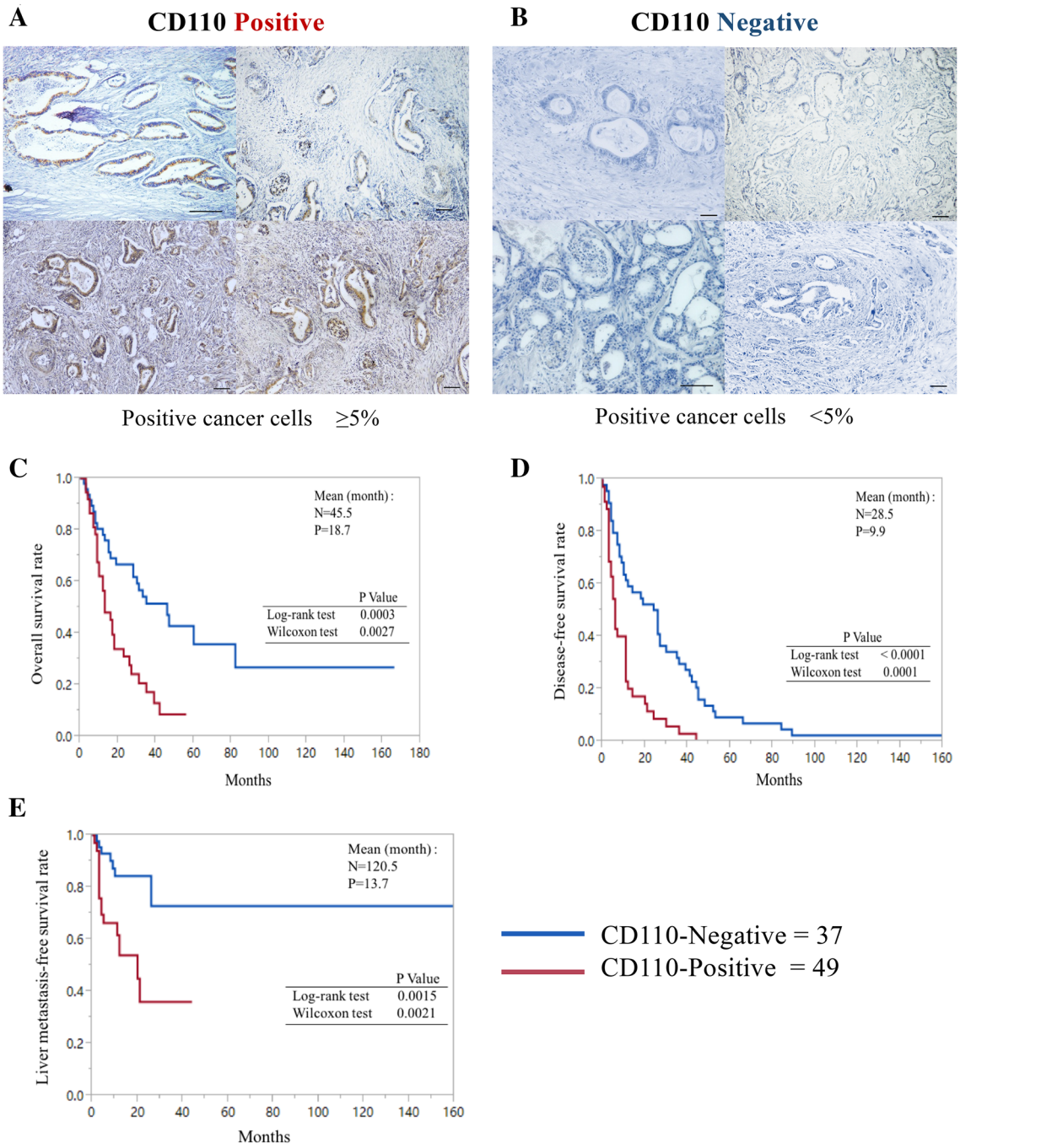

Fig. 6 CD110 expression correlates with poor survival and liver metastasis in PDAC. **a, b** Representative four images of CD110-positive pancreatic tumors (≥5% cells expressing CD110) (A) and CD110-negative pancreatic tumors (**b**). Scale bars = 100 µm. **c** Kaplan–Meier survival analysis of overall survival of pancreatic cancer patients according to CD110 expression. CD110-positive expression was associated with shorter patient survival times (log-rank test, $P = 0.0003$; Wilcoxon test, $P = 0.0027$). **d** Disease-free survival of pancreatic cancer patients according to CD110 expression. CD110-positive expression was associated with shorter disease-free survival times (log rank test, $P < 0.001$; Wilcoxon test, $P = 0.0001$). **e** Liver metastasis-free survival of pancreatic cancer patients according to CD110 expression. CD110-positive expression was associated with shorter time of liver metastasis relapse (log rank test, $P < 0.0015$; Wilcoxon test, $P = 0.0021$)

Table 1 Correlations between CD110 expression and clinicopathologic characteristics

Characteristics	CD110 expression		*P* value
	Positive ($n=37$)	Negative ($n=49$)	
Age			0.0858
≥ 65	29 (78.4%)	30 (61.2%)	
< 65	8 (21.6%)	19 (38.8%)	
Gender			0.8214
Male	21 (56.8%)	29 (59.2%)	
Female	16 (43.2%)	20 (40.8%)	
pT category			0.0019
pT1/pT2	0 (0%)	8 (16.3%)	
pT3/pT4	37 (100%)	41 (83.7%)	
pN category			0.0021
pN0	5 (13.5%)	17 (34.7%)	
pN1	32 (86.5%)	32 (65.3%)	
UICC stage			0.0137
I	0 (0%)	7 (14.3%)	
II	36 (97.3%)	40 (81.6%)	
III/IV	1 (2.7%)	2 (4.1%)	
Histologic grade			0.9757
G1/G2	18 (48.6%)	24 (49.0%)	
G3	19 (51.4%)	25 (51.0%)	
Residual tumor category			0.0115
R0	20 (54.0%)	39 (79.6%)	
R1	17 (46.0%)	10 (20.4%)	
Vessel invasion			0.0082
Positive	29 (78.4%)	25 (51.0%)	
Negative	8 (21.6%)	24 (49.0%)	
Neural invasion			0.1036
Positive	35 (94.6%)	41 (83.7%)	
Negative	2 (5.4%)	8 (16.3%)	
Lymphatic invasion			0.0320
Positive	31 (83.8%)	31 (63.3%)	
Negative	6 (16.2%)	18 (36.7%)	

Table 2 Univariate survival analysis of conventional prognostic factors and CD110 expression

Characteristics	Number of cases	Median OS (months)	*P* value
CD110 expression			0.0003
Positive	37	18.7	
Negative	49	68.0	
Age			0.9784
≥ 65	59	33.5	
< 65	27	58.5	
Gender			0.2694
Male	50	45.9	
Female	36	40.4	
pT category			0.0332
pT1/pT2	8	105.1	
pT3/pT4	78	32.3	
pN category			0.0236
pN0	22	75.8	
pN1	64	30.3	
UICC stage			0.0872
I	7	120.0	
II	76	31.9	
III/IV	3	5.0	
Histologic grade			0.1927
G1/G2	42	53.1	
G3	44	19.9	
Residual tumor category			
R0	59	54.8	
R1	27	19.0	0.0543
Vessel invasion			0.0117
Positive	54	29.7	
Negative	32	66.7	
Neural invasion			0.1646
Positive	76	32.8	
Negative	10	87.0	
Lymphatic invasion			0.0001
Positive	62	27.3	
Negative	24	90.0	

Table 3 Multivariate analysis of conventional prognostic factors and CD110 expression

Characteristics	Relative risk	95% confidence interval	*P* value
Positive CD110 expression	2.107	0.990–3.443	0.0130
pT category pT3 /pT4	1.517	0.471–6.821	0.5109
pN category (pN1)	1.236	0.634–2.646	0.5504
Positive vessel invasion	0.916	0.480–1.815	0.7955
Positive lymphatic invasion	2.799	1.323–6.495	0.0132

Table 4 Correlations between liver metastasis and clinicopathologic characteristics

Characteristics	Liver metastases		*P* value
	Positive ($n=25$)	Negative ($n=61$)	
CD110 expression			0.0422
Positive	15 (60.0%)	22 (36.1%)	
Negative	10 (40.0%)	39 (63.9%)	
Age			0.9384
≥ 65	17 (68.0%)	42 (68.9%)	
< 65	8 (32.0%)	19 (31.1%)	
Gender			0.8214
Male	15 (60.0%)	35 (57.4%)	
Female	10 (40.0%)	26 (42.6%)	
pT category			0.2437
pT1/pT2	1 (4.0%)	7 (11.5%)	
pT3/pT4	24 (96.0%)	54 (88.5%)	
pN category			0.4401
pN0	5 (20.0%)	17 (27.9%)	
pN1	20 (80.0%)	44 (72.1%)	
UICC stage			0.2080
I	1 (4.0%)	6 (9.8%)	
II	24 (96.0%)	52 (85.3%)	
III/IV	0 (0%)	3 (4.9%)	
Histologic grade			0.0026
G1/G2	6 (24.0%)	36 (59.0%)	
G3	19 (76.0%)	25 (41.0%)	
Residual tumor category			0.9384
R0	17 (68.0%)	42 (68.9%)	
R1	8 (32.0%)	19 (31.1%)	
Vessel invasion			0.5196
Positive	17 (68.0%)	37 (60.7%)	
Negative	8 (32.0%)	24 (39.3%)	
Neural invasion			0.9452
Positive	22 (88.0%)	54 (88.5%)	
Negative	3 (12.0%)	7 (11.5%)	
Lymphatic invasion			0.1023
Positive	21 (84.0%)	41 (67.2%)	
Negative	4 (16.0%)	20 (32.8%)	

Table 5 Multivariate analysis of conventional liver metastasis factors and CD110 expression

Characteristics	Relative risk	95% confidence interval	*P* value
CD110 expression			
P/N	0.328	0.098–0.998	0.0498
pT category			
pT1 pT2/pT3 pT4	3.175	0.229–101.179	0.4121
pN category			
pN0/pN1	1.026	0.263–4.431	0.9715
Histologic grade			
G1 G2/G3	4.894	1.635–16.822	0.0040
Residual tumor category			
R0/R1	0.501	0.140–1.630	0.2553
Vessel invasion			
P/N	0.813	0.198–3.346	0.7709
Neural invasion			
P/N	0.432	0.044–3.429	0.4234
Lymphatic invasion			
P/N	1.0962	0.399–11.740	0.4161

Acknowledgements We are grateful to Emiko Manabe and Shoko Sadatomi (Department of Surgery and Oncology, Kyushu University) for skillful technical assistance. Zilong Yan is the recipient of Rotary Yoneyama Memorial Foundation scholarship [http://www.rotary-yoneyama.or.jp]. We thank Edanz Group (http://www.edanzediting.com/ac) for editing a draft of this manuscript. This work was supported by JSPS KAKENHI (Grant number: 26108010, 26293305, 15K10185, 25713050, 16K15621, 16K10601, 16K10600, 16H05417, 15K15498, 15H04933, 16H05418, 17H04284, 17K19602 and 17K19605).

Compliance with ethical standards

Conflict of interest All the authors declare that there is no conflict of interest in this work.

Ethical approval This study was approved by the Kyushu University Institutional Review Board (Fukuoka, Japan).

Informed consent Informed consent was obtained from all individual participants included in the study.

References

Anderberg C et al (2013) Deficiency for endoglin in tumor vasculature weakens the endothelial barrier to metastatic dissemination. J Exp Med 210:563–579. https://doi.org/10.1084/jem.20120662

Bartley TD et al (1994) Identification and cloning of a megakaryocyte growth and development factor that is a ligand for the cytokine receptor. MpI Cell 77:1117–1124. https://doi.org/10.1016/0092-8674(94)90450-2

Besancenot R et al (2010) A senescence-like cell-cycle arrest occurs during megakaryocytic maturation: implications for physiological and pathological megakaryocytic proliferation PLoS Biol. https://doi.org/10.1371/journal.pbio.1000476

Besancenot R et al (2014) JAK2 and MPL protein levels determine TPO-induced megakaryocyte proliferation vs differentiation. Blood 124:2104–2115. https://doi.org/10.1182/blood-2014-03-559815

Chabottaux V et al (2009) Membrane-type 4 matrix metalloproteinase (MT4-MMP) induces lung metastasis by alteration of primary breast tumour vascular architecture. J Cell Mol Med 13:4002–4013. https://doi.org/10.1111/j.1582-4934.2009.00764.x

Chanprasert S, Geddis AE, Barroga C, Fox NE, Kaushansky K (2006) Thrombopoietin (TPO) induces c-myc expression through a PI3K- and MAPK-dependent pathway that is not mediated by Akt, PKC-zeta or mTOR in TPO-dependent cell lines and primary megakaryocytes. Cell Signal 18:1212–1218. https://doi.org/10.1016/j.cellsig.2005.09.010

Chijiiwa Y et al (2016) Overexpression of microRNA-5100 decreases the aggressive phenotype of pancreatic cancer cells by targeting PODXL. Int J Oncol 48:1688–1700. https://doi.org/10.3892/ijo.2016.3389

Choi C, Helfman DM (2014) The Ras-ERK pathway modulates cytoskeleton organization, cell motility and lung metastasis signature genes in MDA-MB-231. LM2 Oncogene 33:3668–3676. https://doi.org/10.1038/onc.2013.341

Dong-Feng Z, Ting L, Yong Z, Cheng C, Xi Z, Pei-Yan K (2014) The TPO/c-MPL pathway in the bone marrow may protect leukemia cells from chemotherapy in AML Patients. Pathol Oncol Res 20:309–317. https://doi.org/10.1007/s12253-013-9696-z

Dorsch M, Fan P-D, Danial NN, Rothman PB, Goff SP (1997) The thrombopoietin receptor can mediate proliferation without activation of the Jak-STAT pathway. J Exp Med 186:1947–1955

Elf S et al (2016) Mutant calreticulin requires both its mutant C-terminus and the thrombopoietin receptor for oncogenic transformation. Cancer Discov 6:368–381. https://doi.org/10.1158/2159-8290.CD-15-1434

Engl T et al (2006) CXCR4 chemokine receptor mediates prostate tumor cell adhesion through alpha5 and beta3 integrins. Neoplasia 8:290–301. https://doi.org/10.1593/neo.05694

Gao W, Chen L, Ma Z, Du Z, Zhao Z, Hu Z, Li Q (2013) Isolation and phenotypic characterization of colorectal cancer stem cells with organ-specific metastatic potential. Gastroenterology 145:636–646 e635. https://doi.org/10.1053/j.gastro.2013.05.049

Gleisner AL et al (2007) Is resection of periampullary or pancreatic adenocarcinoma with synchronous hepatic metastasis justified? Cancer 110:2484–2492. https://doi.org/10.1002/cncr.23074

Goetz JG et al (2011) Biomechanical remodeling of the microenvironment by stromal caveolin-1 favors tumor invasion and metastasis. Cell 146:148–163. https://doi.org/10.1016/j.cell.2011.05.040

Hayes TK et al (2016) Long-term ERK Inhibition in KRAS-mutant pancreatic cancer is associated with myc degradation and senescence-like growth suppression. Cancer Cell 29:75–89. https://doi.org/10.1016/j.ccell.2015.11.011

Hess KR, Varadhachary GR, Taylor SH, Wei W, Raber MN, Lenzi R, Abbruzzese JL (2006) Metastatic patterns in adenocarcinoma. Cancer 106:1624–1633. https://doi.org/10.1002/cncr.21778

Hitchcock IS, Kaushansky K (2014) Thrombopoietin from beginning to end. Br J Haematol 165:259–268. https://doi.org/10.1111/bjh.12772

Kaushansky K (2005) The molecular mechanisms that control thrombopoiesis. J Clin Invest 115:3339–3347. https://doi.org/10.1172/JCI26674

Kaushansky K (2006) Lineage-specific hematopoietic growth factors. N Engl J Med 354:2034–2045. https://doi.org/10.1056/NEJMra052706

Kukreja P, Abdel-Mageed AB, Mondal D, Liu K, Agrawal KC (2005) Up-regulation of CXCR4 expression in PC-3 cells by stromal-derived factor-1alpha (CXCL12) increases endothelial adhesion and transendothelial migration: role of MEK/ERK signaling pathway-dependent NF-kappaB activation. Cancer Res 65:9891–9898. https://doi.org/10.1158/0008-5472.CAN-05-1293

Lin WC et al (2013) Dormant cancer cells contribute to residual disease in a model of reversible pancreatic cancer. Cancer Res 73:1821–1830. https://doi.org/10.1158/0008-5472.CAN-12-2067

Lok S et al (1994) Cloning and expression of murine thrombopoietin cDNA and stimulation of platelet production in vivo. Nature 369:565. https://doi.org/10.1038/369565a0

Moriyama T, Ohuchida K, Mizumoto K, Cui L, Ikenaga N, Sato N, Tanaka M (2010) Enhanced cell migration and invasion of CD133 + pancreatic cancer cells cocultured with pancreatic stromal cells. Cancer 116:3357–3368. https://doi.org/10.1002/cncr.25121

Morris EJ et al (2013) Discovery of a novel ERK inhibitor with activity in models of acquired resistance to BRAF and MEK inhibitors. Cancer Discov 3:742–750. https://doi.org/10.1158/2159-8290.CD-13-0070

Neyaz A et al (2018) Investigation of targetable predictive and prognostic markers in gallbladder carcinoma. J Gastrointest Oncol 9:111–125. https://doi.org/10.21037/jgo.2017.10.02

Noone AM, Cronin KA, Altekruse SF, Howlader N, Lewis DR, Petkov VI, Penberthy L (2017) Cancer incidence and survival trends by subtype using data from the surveillance epidemiology and end results program, 1992–2013. Cancer Epidemiol Biomark Prev 26:632–641. https://doi.org/10.1158/1055-9965.EPI-16-0520

Palomero T et al (2006) NOTCH1 directly regulates c-MYC and activates a feed-forward-loop transcriptional network promoting leukemic cell growth. Proc Natl Acad Sci USA 103:18261–18266. https://doi.org/10.1073/pnas.0606108103

Pikman Y et al (2006) MPLW515L is a novel somatic activating mutation in myelofibrosis with myeloid metaplasia. PLoS Med 3:e270. https://doi.org/10.1371/journal.pmed.0030270

Principe DR et al (2017) TGFbeta engages MEK/ERK to differentially regulate benign and malignant pancreas cell function. Oncogene 36:4336–4348. https://doi.org/10.1038/onc.2016.500

Qian BZ et al (2011) CCL2 recruits inflammatory monocytes to facilitate breast-tumour metastasis. Nature 475:222–225. https://doi.org/10.1038/nature10138

Reymond N et al (2012) Cdc42 promotes transendothelial migration of cancer cells through beta1 integrin. J Cell Biol 199:653–668. https://doi.org/10.1083/jcb.201205169

Reymond N, d'Água BB, Ridley AJ (2013) Crossing the endothelial barrier during metastasis. Nat Rev Cancer 13:858–870. https://doi.org/10.1038/nrc3628

Rojnuckarin P, Drachman JG, Kaushansky K (1999) Thrombopoietin-induced activation of the mitogen-activated protein kinase (MAPK) pathway in normal megakaryocytes: role in endomitosis. Blood 94:1273

Rouyez MC, Boucheron C, Gisselbrecht S, Dusanter-Fourt I, Porteu F (1997) Control of thrombopoietin-induced megakaryocytic differentiation by the mitogen-activated protein kinase pathway. Mol Cell Biol 17:4991–5000

Roy LD et al (2011) MUC1 enhances invasiveness of pancreatic cancer cells by inducing epithelial to mesenchymal transition. Oncogene 30:1449–1459. https://doi.org/10.1038/onc.2010.526

Sakamoto A et al (2016) Live-cell single-molecule imaging of the cytokine receptor MPL for analysis of dynamic dimerization. J Mol Cell Biol 8:553–555. https://doi.org/10.1093/jmcb/mjw027

Sangkhae V, Etheridge SL, Kaushansky K, Hitchcock IS (2014) The thrombopoietin receptor, MPL, is critical for development of a JAK2V617F-induced myeloproliferative neoplasm. Blood 124:3956–3963. https://doi.org/10.1182/blood-2014-07-587238

Sato N, Maehara N, Goggins M (2004) Gene expression profiling of tumor–stromal interactions between pancreatic cancer cells and stromal fibroblasts. Cancer Res 64:6950

Sears R, Nuckolls F, Haura E, Taya Y, Tamai K, Nevins JR (2000) Multiple Ras-dependent phosphorylation pathways regulate Myc protein stability. Genes Dev 14:2501–2514

Sheng W et al (2017) Calreticulin promotes EGF-induced EMT in pancreatic cancer cells via Integrin/EGFR-ERK/MAPK signaling pathway. Cell Death Dis 8:e3147. https://doi.org/10.1038/cddis.2017.547

Steeg PS (2006) Tumor metastasis: mechanistic insights and clinical challenges. Nat Med 12:895–904. https://doi.org/10.1038/nm1469

Stewart BW, Wild C, International Agency for Research on Cancer, World Health Organization (2014) World cancer report 2014. International Agency for Research on Cancer

Talmadge JE, Fidler IJ (2010) AACR centennial series: the biology of cancer metastasis: historical perspective. Cancer Res 70:5649–5669. https://doi.org/10.1158/0008-5472.CAN-10-1040

Tichet M et al (2015) Tumour-derived SPARC drives vascular permeability and extravasation through endothelial VCAM1 signalling to promote metastasis. Nat Commun 6:6993. https://doi.org/10.1038/ncomms7993

Tsai WB, Aiba I, Long Y, Lin HK, Feun L, Savaraj N, Kuo MT (2012) Activation of Ras/PI3K/ERK pathway induces c-Myc stabilization to upregulate argininosuccinate synthetase, leading to arginine deiminase resistance in melanoma cells. Cancer Res 72:2622–2633. https://doi.org/10.1158/0008-5472.CAN-11-3605

Vaseva AV et al (2018) KRAS suppression-induced degradation of MYC Is antagonized by a MEK5-ERK5 compensatory. Mech Cancer Cell 34:807–807+. https://doi.org/10.1016/j.ccell.2018.10.001

Wang X, Cunningham M, Zhang X, Tokarz S, Laraway B, Troxell M, Sears RC (2011) Phosphorylation regulates c-Myc's oncogenic activity in the mammary gland. Cancer Res 71:925–936. https://doi.org/10.1158/0008-5472.CAN-10-1032

Wendel C, Hemping-Bovenkerk A, Krasnyanska J, Mees ST, Kochetkova M, Stoeppeler S, Haier J (2012) CXCR4/CXCL12 participate in extravasation of metastasizing breast cancer cells within the liver in a rat model. PLoS One 7:e30046. https://doi.org/10.1371/journal.pone.0030046

Weng AP et al (2006) c-Myc is an important direct target of Notch1 in T-cell acute lymphoblastic leukemia/lymphoma. Genes Dev 20:2096–2109. https://doi.org/10.1101/gad.1450406

Wu Z et al (2015) TPO-induced metabolic reprogramming drives liver metastasis of colorectal cancer CD110 + tumor-initiating cells. Cell Stem Cell 17:47–59. https://doi.org/10.1016/j.stem.2015.05.016

Yamazaki H, Nishida H, Iwata S, Dang NH, Morimoto C (2009) CD90 and CD110 correlate with cancer stem cell potentials in human T-acute lymphoblastic leukemia cells. Biochem Biophys Res Commun 383:172–177. https://doi.org/10.1016/j.bbrc.2009.03.127

Zabel BA et al (2009) Elucidation of CXCR7-mediated signaling events and inhibition of CXCR4-mediated tumor cell transendothelial migration by CXCR7 ligands. J Immunol 183:3204–3211. https://doi.org/10.4049/jimmunol.0900269

Zheng B et al (2016) CD146 attenuation in cancer-associated fibroblasts promotes pancreatic cancer progression. Mol Carcinog 55:1560–1572. https://doi.org/10.1002/mc.22409